How to cite: *Angew. Chem. Int. Ed.* **2023**, *62*, e202314378
doi.org/10.1002/anie.202314378

Cage Structures

A Lantern-Shaped Pd(II) Cage Constructed from Four Different Low-Symmetry Ligands with Positional and Orientational Control: An Ancillary Pairings Approach

Dan Preston and Jack D. Evans*

Abstract: One of the key challenges of metallo-supramolecular chemistry is to maintain the ease of self-assembly but, at the same time, create structures of increasingly high levels of complexity. In palladium(II) quadruply stranded lantern-shaped cages, this has been achieved through either 1) the formation of heteroleptic (multi-ligand) assemblies, or 2) homoleptic assemblies from low-symmetry ligands. Heteroleptic cages formed from low-symmetry ligands, a hybid of these two approaches, would add an additional rich level of complexity but no examples of these have been reported. Here we use a system of ancillary complementary ligand pairings at the termini of cage ligands to target heteroleptic assemblies: these complementary pairs can only interact (through coordination to a single Pd(II) metal ion) between ligands in a *cis* position on the cage. Complementarity between each pair (and orthogonality to other pairs) is controlled by denticity (tridentate to monodentate or bidentate to bidentate) and/or hydrogen-bonding capability (AA to DD or AD to DA). This allows positional and orientational control over ligands with different ancillary sites. By using this approach, we have successfully used low-symmetry ligands to synthesise complex heteroleptic cages, including an example with four different low-symmetry ligands.

[*] Dr. D. Preston
Research School of Chemistry, Australian National University
Canberra, ACT 2600 (Australia)
E-mail: daniel.preston@anu.edu.au

Dr. J. D. Evans
Centre for Advanced Nanomaterials and Department of Chemistry, The University of Adelaide
Adelaide, SA 5000 (Australia)

Introduction

Chemists have demonstrated success in creating bio-mimetic structures using self-assembly techniques, such as the formation of metallo-supramolecular cages,[1] which can resemble, in some ways, the structure of proteins. However a distinct limitation of these synthetic systems has been their high symmetry compared to the diverse sequences and varied structures observed in Nature. This lowers their potential specificity towards molecular targets. A lot of work has gone into overcoming this problem, much of it centring on quadruply stranded palladium(II) lantern-shaped cages, first synthesised in homoleptic, high-symmetry form by McMorran and Steel[2] (Figure 1A), using simple ditopic ligands in which the directional angles ofthe donor atoms align in parallel to one another.

Two distinct strategies have emerged to access lower symmetry lantern-shaped cages. The first of these is the successful integration of multiple ligands into a unified heteroleptic structure.[3] For this approach to be effective, positional control must be achieved. A variety of driving forces for positional control have been used including endohedral sterics in the formation of a 3:1 heteroleptic cage[4] (Figure 1G), sterics and hydrogen bonding in exohedral amino groups in the formation of a 2:2 *cis* heteroleptic cage[5] (Figure 1H), sterics with exohedral clash between quinoline groups for a 3:1 heteroleptic cage[6] (Figure 1I), and the combination of endo- and exo-steric bulk for the formation of a 2:1:1 heteroleptic cage[7] (Figure 1J). Alternatively, for heteroleptic cage formation, the principle of geometric complementarity can be employed where ligands have complementarity 'bite' angles between their donor groups, i.e. one more open than parallel, and the other (with a suitably lengthened backbone) more closed. Using this approach, both 2:2 *cis*[8] (Figure 1K) and 2:2 *trans*[9] structures have been obtained.[10]

The second approach has been the use of a single type of low-symmetry ligand with distinguishable 'ends'. The combination of a low-symmetry ligand with palladium(II) can result in the formation of a lower symmetry lantern-shaped cage.[11] Here, effectiveness requires orientational control, and this has likewise been imparted by sterics[12] (*trans* isomer, Figure 1B), sterics and hydrogen bonding[13] (*cis* isomer, Figure 1C), and geometric complementarity in a low-symmetry ligand[11,14] (*cis*, Figure 1D).[15] Interesting work from Lewis linked two low-symmetry ligands together at their peripheries with organic chemistry, allowing the use

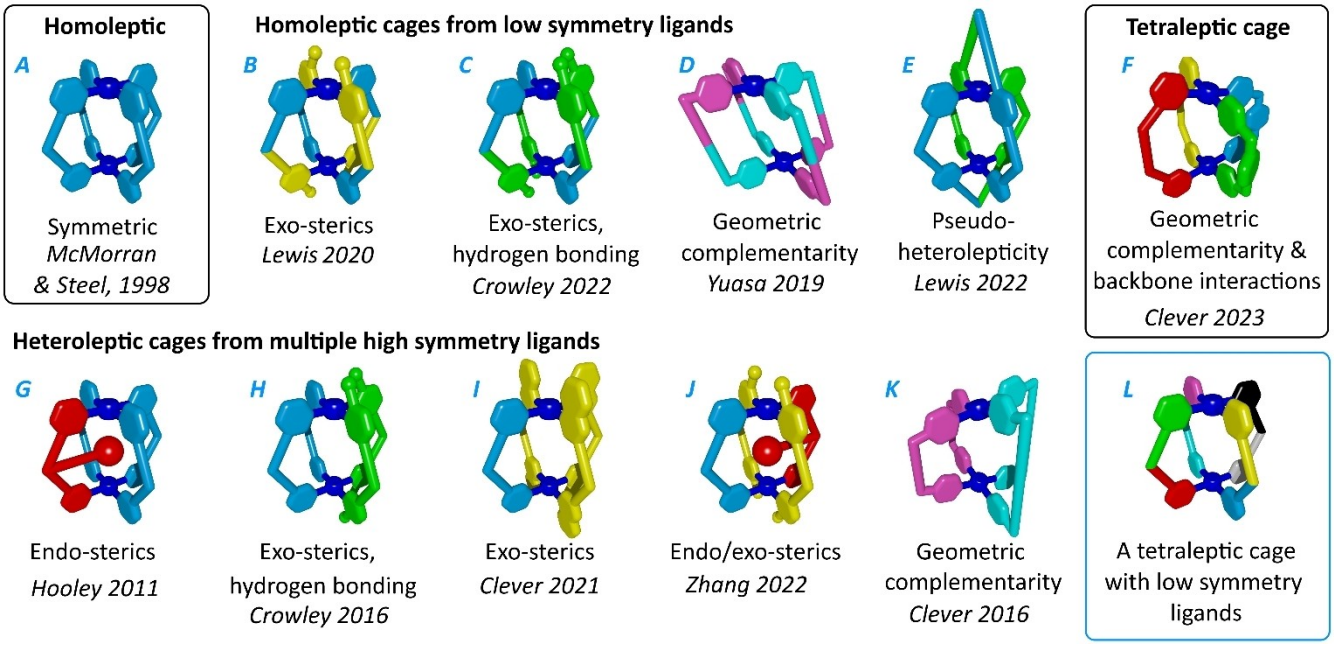

Figure 1. Different approaches to generating low-symmetry systems in lantern-shaped cages either as homoleptic low-symmetry cages or heteroleptic cages. A proposed heteroleptic low-symmetry ligand cage target is shown in the blue inset. The date and author of the first report are shown where appropriate.

of low-symmetry ligands to form pseudo-heteroleptic cages (Figure 1E).[16]

Of all these approaches, the greatest singular success has been reported by Clever and co-workers, who successfully synthesised a number of heteroleptic cages with four different ligands.[17] Their approach relied upon favourable CH-π interactions between two of the ligands (e.g. green and blue, Figure 1F) driving these into a *cis* orientation with respect to one another, while the other two ligands (yellow and red) have geometric complementarity to the first two. Hiroaka and co-workers have recently used kinetic control to also access different varieties of heteroleptic structures.[18]

However, what has not been accomplished has been the formation of lantern-shaped cages which combine these two approaches, and so are both heteroleptic and formed from low-symmetry ligands. The apex of this particular approach would be a tetraleptic cage with four low-symmetry ligands, over each of which with positional and orientational control (Figure 1L). This achievement would enable the potential for integration of a significantly higher level of complexity.

While we have done some work on cages, including heteroleptic ones,[19] most of our endeavours have been focussing on generation of structural complexity through other means and in other structures. We have been inspired by the control Nature achieves through the formation of sequences, and have strived to create our own self-assembled defined sequences, using ligand pairings, where two ligands come together at a square planar metal ion such as Pd(II) in a complementary fashion (Figure 2a).[20] This complementarity can be driven by the respective denticities of the ligands (tridentate complementary to monodentate (3:1), or bidentate to bidentate (2:2)), or by hydrogen bonding analogous to that between DNA base pairs (site 2_{AA} with two hydrogen bond acceptors, has complementarity to site 2_{DD} with two hydrogen bond donors, while site 2_{AD} is complementary to 2_{DA}).[21] We have demonstrated that these pairings can be integrated into assemblies to direct structure,[22] and can be used orthogonally to one another in a single system.[23] We contemplated the fact that Nature forms low-symmetry environments in proteins through formation of a varied sequence that then assembles into a 3-dimensional structure (Figure 2b), and envisaged a sequence formed with our pairings that incorporated ditopic ligands, for the formation of heteroleptic cages with low-symmetry ligands. This report details this work, including the first example of a lantern-shaped palladium(II) cage formed from four different low-symmetry ligands.

Results and Discussion

All ligands were synthesised and characterised using standard approaches (Supporting Information, S1.2 and S1.3). All ligands were comprised of a simple dipyridyl core with a 1,3-diethynylbenzene linker (exemplified by ligand **0**, Figure 2c), which has previously been used in the construction of lantern-shaped cages[24] and exploration of their function and behaviour.[25] The use of this simple ligand core was by design, to show in proof-of-concept that any structural control obtained was solely through our ancillary pairings approach.

One of the pyridyl groups of this dipyridyl core was in some cases decorated with one member from our three complementary pairings (Figure 2c). For example, ligand **3**

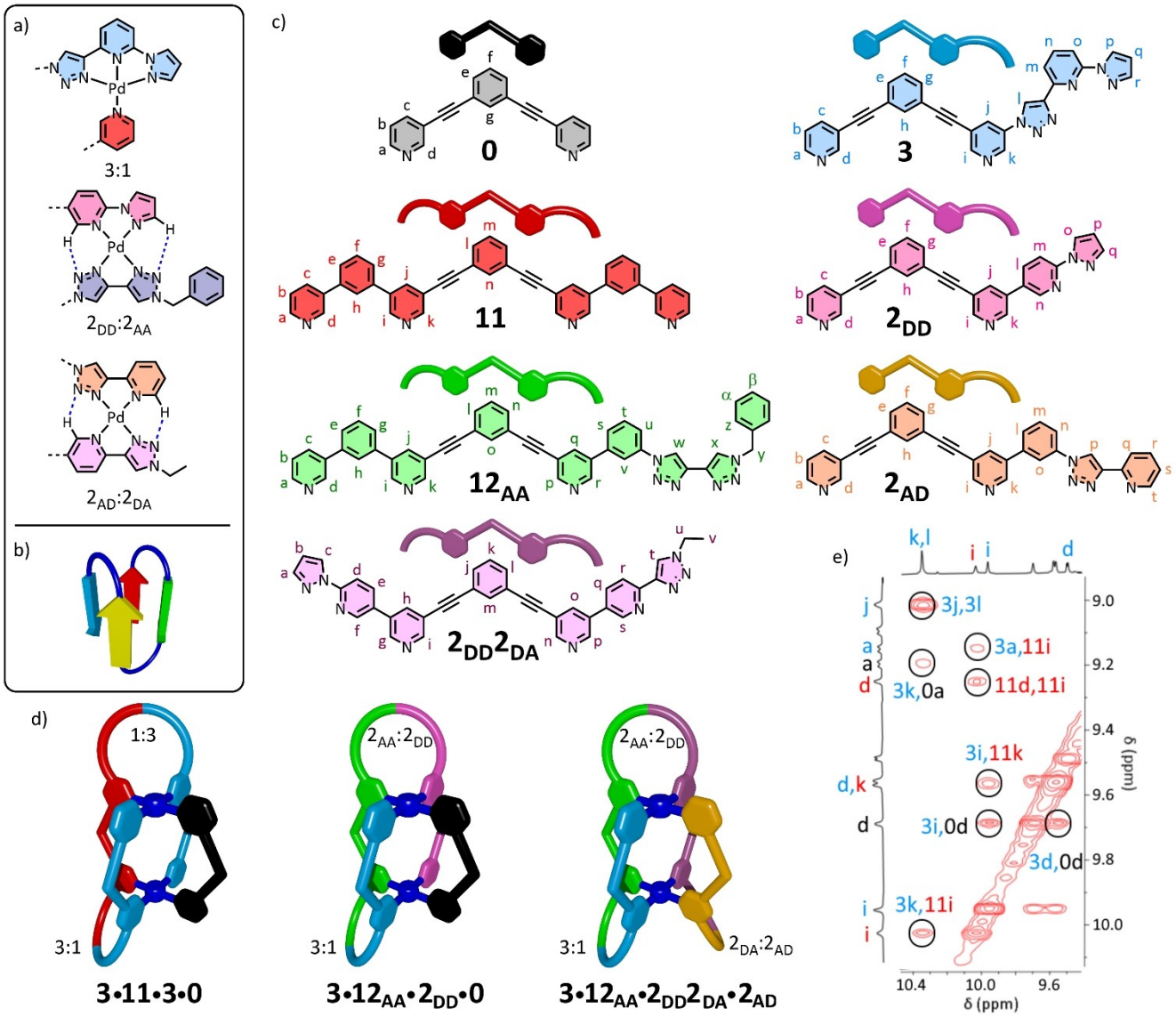

Figure 2. a) The complementary ligand pairings used in this study. b) A schematic representation of a molecular sequence forming a low-symmetry environment. c) Labelled structures of the ligands used in this study. d) Schematic representations of the heteroleptic low-symmetry lantern-shaped cages formed from the different combinations of these ligands with palladium(II). e) Partial ^{1}H NOESY NMR spectrum (400 MHz, [D$_6$]DMSO, 298 K, 200 ms) of cage **3·11·3·0**.

had at one end a tridentate site, while ligand $\mathbf{2_{DD}}$ has one end functionalised with the 2_{DD} site. Other ligands are decorated at both ends, for example ligand $\mathbf{12_{AA}}$ had a monodentate site attached at one end, and a 2_{AA} site at the other. Different ligands therefore had sites ancillary to the dipyridyl core capable of coordinating to a palladium(II) metal ion in a complementary fashion, i.e. 3:1, 2_{AA}:2_{DD} and 2_{AD}:2_{DA}. Furthermore, ligands were designed to place geometric constraints on ligands interacting with one another through a pairing, with design led by early modelling. By way of example, the tridentate site on ligand **3** can occupy three of the four sites on a palladium(II) metal ion. A monodentate site (such as at either end of ligand **11** for example) can occupy the fourth and final site on the palladium(II) metal ion, but in order to be able to 'reach' the metal ion, ligands **3** and **11** need to be *cis* to one another with respect to their position in the lantern-shaped cage: if *trans* to each other, then the two sites will be too far apart. In addition to the requirement to be positioned *cis* to one another, the appropriate ligands must also be orientated with the ancillary sites at the same end of the cage. We thereby hoped to control both orientation and position of different combinations of ligands within their lantern-shaped cages.

With our ligands in hand and a strategy prepared, we first targeted the formation of a cage with three different ligands. Ligand **11** has two monodentate sites, one at each end. Two equivalents of ligand **3** were therefore required, to give two 3:1 pairings. The requirement that ligands need be *cis* to one another for the complementary pairings to be able

to connect was intended to drive the two equivalents of **3** into the two positions *cis* to ligand **11**, and therefore *trans* to one another (Figure 2d), with a head-to-tail orientation towards one another as they each interact with one of the two monodentate sites at either end of **11**. The fourth ligand **0** with no ancillary pairing capability was hoped to occupy the final ligand site on the cage, as any other ligand in this site would require a thermodynamic sacrifice. This thermodynamic sacrifice could conceivably be enthalpic (a severed ancillary pairing) and to get a measure of the thermodynamic cost we computed the structure and energies of the proposed **3·11·3·0** cage and its separate constituents (Density Functional Theory (DFT) calculations, BP86 functional, C and H atoms treated with the def2-SVP basis set, all other atoms with the def2-TZVPP basis set), and calculated the free energy of formation as $-458\,kJ\,mol^{-1}$. In comparison, our calculations for the 'simple' homoleptic cage $[Pd_2(\mathbf{0})_4]^{4+}$ gave the enthalpy of formation as $-280\,kJ\,mol^{-1}$, unsurprisingly showing that maximal binding site occupancy of added pairings leads to significant higher enthalpic stability. It would be presumably possible to circumvent this through linking two lantern shaped cages or other large assemblies into a single structure, but this would carry an entropic burden. We therefore felt confident that our strategy would give the **3·11·3·0** as the significantly favoured thermodynamic product.

In [D_6]DMSO, ligands **3**, **11** and **0** in a 2:1:1 ratio were combined with 4 equivalents of $[Pd(CH_3CN)_4](BF_4)_2$, two for the cage structure and one for each 3:1 pairing present. After heating at 40 °C for 6 hours, no additional spectral changes were observed. High resolution electrospray ionisation mass spectrometry (HR-ESI MS) on the sample revealed signals associated with a species with the three ligands in the desired 2:1:1 ratio, for example $[Pd_4(\mathbf{3})_2(\mathbf{11})(\mathbf{0})](BF_4)_5^{3+}$ at $m/z = 902.0954$ (Supporting Information, Figure S1.38). No other ligand combinations were observed in intact cages in the spectrum.

The combination of two high-symmetry ligands and two equivalents of a low symmetry ligand in a quadruply stranded lantern-shaped cage can potentially result in four combinations of position and orientation, excluding spectroscopically equivalent enantiomers (Figure 3a). The two equivalents of the low-symmetry ligand can either be positioned *cis* or *trans* to one another, and can be orientated in either a head-to-head or head-to-tail manner with respect to one another. These different combinations impact on the degree of symmetry (or lack thereof) exhibited by each ligand, and only the *trans* head-to-tail species has a single ligand environment per ligand.

In the ^{1}H NMR spectrum (Figure 4a), only a single set of signals per ligand environment was observed, at downfield chemical shifts from those in spectra of the 'free' ligands. From this symmetry a number of conclusions about the structure could be deduced: 1) The ligands combine to form a structure as a single enantiomeric pair, 2) The single environment for ligand **3** shows that the two equivalents of this ligand are *trans* to one another. If they were *cis*, they would be adjacent to different ligands, one to **0** and one to **11**, and would be in different chemical environments (Figure 3). Additionally, 3) the two equivalents of ligand **3** are orientated in a head-to-tail fashion to one another. If they were head-to-head, the respective ends of ligands **0** and **11** would each become chemically inequivalent. Therefore, the symmetry exhibited in the ^{1}H NMR spectrum was consistent with our intended structure.

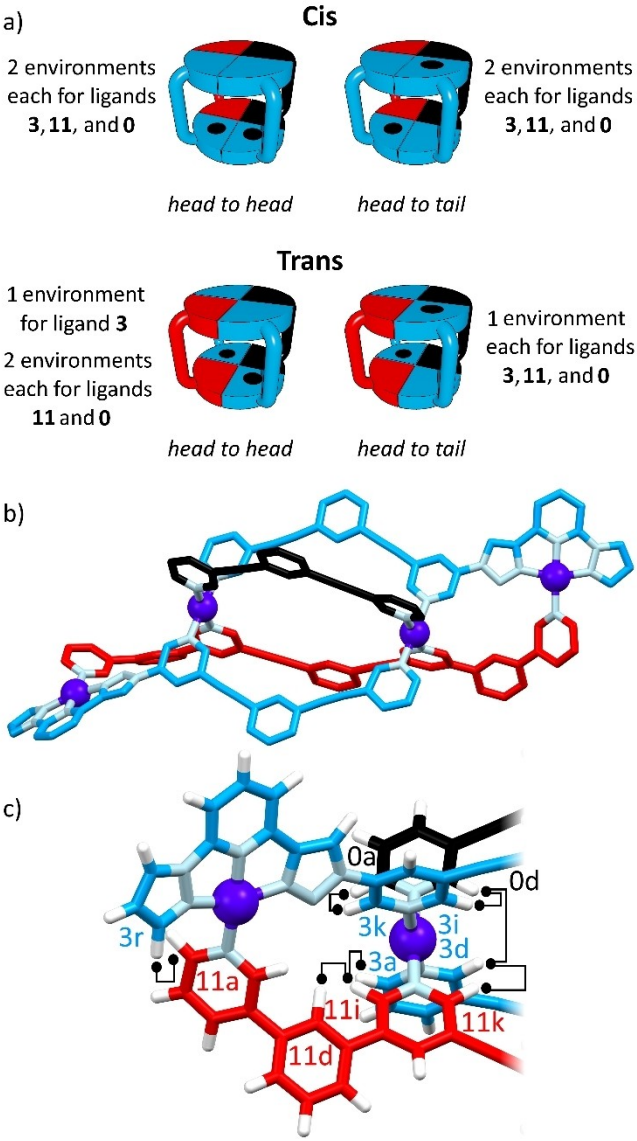

Figure 3. a) Schematic representation of possible positional and orientational combinations of two equivalents of low-symmetry ligand **3** (blue, with the different ends of the ligand distinguished with black dots), and one equivalent respectively of high-symmetry ligands **11** (red) and **0** (black). The two equivalents of ligand **3** can be *cis* or *trans* to one another, and be orientated either head to head or head to tail. The consequences of each combination on the symmetry of the environments of the ligands are also noted. b) DFT-calculated structure of **3·11·3·0**, ligands same colour as in (a), nitrogen atoms light blue, palladium atoms dark blue, some hydrogen atoms are omitted. c) Section of this cage with key diagnostic NOE correlations mapped onto the structure.

We next examined the 2D Nuclear Overhauser Effect Spectroscopy (NOESY)[26] NMR spectrum of the complex

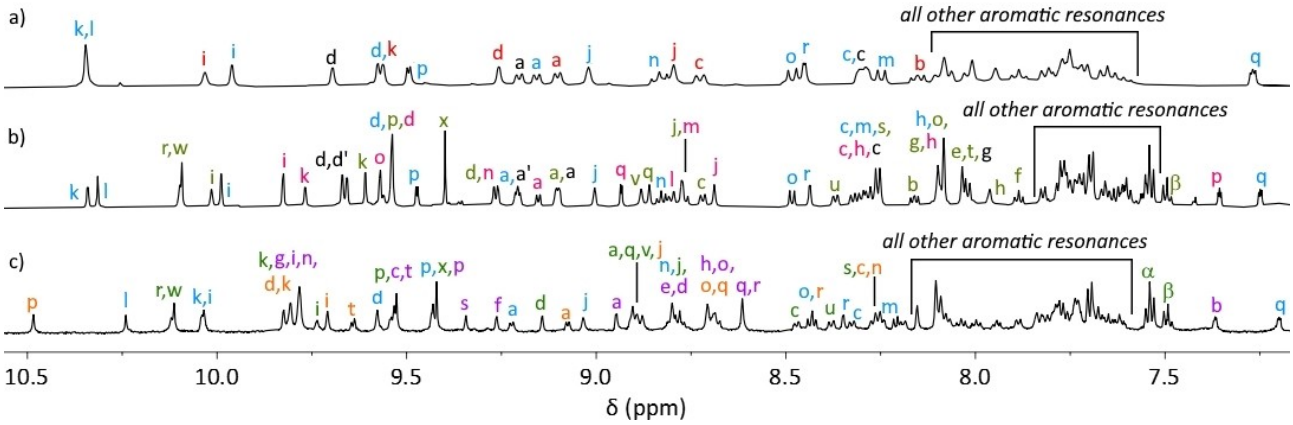

Figure 4. Partial stacked ^{1}H NMR spectra (600 MHz, [D$_6$]DMSO, 298 K) of a) **3**·**11**·**3**·**0** (label colours: **3** blue, **11** red, **0** black), b) **3**·$\mathbf{12_{AA}}$·$\mathbf{2_{DD}}$·**0** (label colours: **3** blue, $\mathbf{12_{AA}}$ green, $\mathbf{2_{DD}}$ pink, **0** black), and c) **3**·$\mathbf{2_{AA}}$·$\mathbf{2_{DD}}\mathbf{2_{DA}}$·$\mathbf{2_{AD}}$ (label colours: **3** blue, $\mathbf{12_{AA}}$ green, $\mathbf{2_{DD}}\mathbf{2_{DA}}$ purple, $\mathbf{2_{AD}}$ orange, **0** black). Proton labelling shown in Figure 2.

(Figure 2e). In lantern-shaped cages, the protons *ortho* to coordinating nitrogen atoms of a given ligand (for example, environments *a* and *d* of ligand **0**) are approximately 3.1 Å away from the equivalent *ortho* protons on the ligand *cis* to the first. A *trans* relationship sees this distance increase to approximately 4.4 Å.[27] This greater nuclear separation results in an eightfold decrease in correlation strength[28] between *trans* and *cis* ligand environments (all other things being equal) and so NOE correlations can be used to reliably determine *cis* arrangements between proton resonances of ligands in lantern-shaped cages.[5a,17]

A series of correlations were observed consistent with (and only consistent with) the ligands being present in the intended positions and orientations. For example, the endohedral proton ortho to coordinating nitrogen atoms in ligand **0** (*d*) showed correlations to environments *d* and *i* of ligand **3**, confirming the *trans* and head-to-tail position and orientation of the two equivalents of ligand **3** with respect to one another. Likewise, the exohedral proton ortho (*i*) to the coordinating nitrogens of ligand **11** was correlated to exohedral environments from both ends of ligand **3**, *a* and *k*, confirming the *cis* position of **11** to both equivalents of ligand **3**, again in a head-to-tail orientation. Confirmation of the presence of both components of the 3:1 pairing in spatial proximity was also evident in the correlation between environment *r* from the tridentate site of **3** and *a* from the monodentate site of **11**.

Additional conformation was given by ^{1}H Diffusion Ordered (DOSY) NMR spectroscopy. The assorted free ligands synthesised in this project have diffusion coefficients of 1.4–2.3×10^{-10} m^{2}s^{-1}. All of the signals in the spectrum of this assembly were diffusing at the same rate, indicating formation of a single assembly, and this rate (0.68×10^{-10} m^{2}s^{-1}) was slower than the free ligands, indicating formation of a larger architecture. The thrust of the conclusions from the DOSY data were replicated in other subsequent cages formed in this study (Supporting Information).[29]

Despite our best efforts, attempts to obtain X-ray quality crystals of this or other complexes formed in this study were unsuccessful. However, the data allow clear conclusions to be drawn on the solution-phase structure of this compound. In all, the data can only be reasonably explained by the formation of a trileptic lantern shaped cage, with two symmetric ligands (**0** and **11**) *trans* to one another, and the two equivalents of low-symmetry ligand **3** also *trans* to one another and with head-to-tail orientation. Our previously obtained DFT calculations showed that this structure was feasible (Figure 3b). Using this structure, we were able to make comparison to the NOE correlations observed, confirming that they were consistent with our proposed positioning and orientation of ligands within the structure (Figure 3c).

Having established that our design could ensure that ligands with complementary pairings could be constrained to *cis* orientations with respect to one another in lantern-shaped cages, we next sought to demonstrate that different pairings could be incorporated into a single assembly, to generate enhanced structural variety. Previously, we used ligand **11** with two ancillary monodentate sites. Now we used instead ligand $\mathbf{12_{AA}}$ (Figure 2c) with one monodentate site and one 2_{AA} site. One equivalent of ligand **3** was used (3:1 pairing) while ligand $\mathbf{2_{DD}}$ was now incorporated, with complementarity towards the 2_{AA} site of $\mathbf{12_{AA}}$. As before the final ligand in the cage was intended to be ligand **0**, with no ancillary capability. The *cis* requirement for paired ancillary groups was therefore intended to have both ligands **3** and $\mathbf{2_{DD}}$ *cis* to ligand $\mathbf{12_{AA}}$ (and therefore *trans* to one another, in a head-to-tail fashion with respect their unsubstituted ends) and ligand **0** in the last position, *trans* to ligand $\mathbf{12_{AA}}$ (cartoon shown in Figure 2d). The four ligands were combined in a 1:1:1:1 ratio, together with 4 equivalents of the Pd(II) source, in [D$_6$]DMSO, with gentle heating at 40 °C for six hours. HR ESI mass spectral analysis confirmed the presence of a species with the desired composition, $[Pd_4(\mathbf{3})(\mathbf{12_{AA}})(\mathbf{2_{DD}})(\mathbf{0})]^{8+}$, together with associated anions, for example $m/z = 1437.1250$, for $[\mathbf{M}+6BF_4^-]^{2+}$ (Supporting

Information, Figure S1.46). The ^{1}H NMR spectrum showed that signals were downfield shifted with respect to 'free' ligands, indicating coordination (Figure 4b). There was one set of signals for each ligand environment *except* ligand **0** which had been desymmetrised into two halves. This is consistent with the formation of a single enantiomeric pair, with the two ends of **0** now in different environments with the introduction of two ancillary pairings. The desired control over ligand position and orientation could be demonstrated through the 2D NOESY NMR correlations.

For example, environment *k* of ligand $\mathbf{12_{AA}}$ was correlated to *i* from **3**, showing their *cis* positioning and that their monodentate and tridentate ancillary sites were both orientated at the same 'end' of the cage. Meanwhile, there was correlation between site *r* of $\mathbf{12_{AA}}$ and site *k* of $\mathbf{2_{DD}}$, confirming that ligand $\mathbf{2_{DD}}$ occupied the other position *cis* to $\mathbf{12_{AA}}$, and was head-to-tail with ligand **3**. Again, spatial proximity between ancillary pairings could also be established through NOE correlations: for 3:1, between environment *r* of **3** and *a* of $\mathbf{12_{AA}}$, and for 2_{AA}:2_{DD}, between methylene environment *y* of $\mathbf{12_{AA}}$ and environment *q* of ligand $\mathbf{2_{DD}}$ (Supporting Information, Figues S1.41, S1.42, S1.3), hence connectivity, positioning and orientation between ligands was being driven through the ancillary pairings system. Again, a computationally derived structure showed that not only was this orientation and positioning of ligands feasible, but that it mapped with the observed NOE correlations (Figure 5a, b and c).

Synthesis of $\mathbf{3{\cdot}12_{AA}{\cdot}2_{DD}{\cdot}0}$ had shown that the 3:1 and 2_{DD}:2_{AA} ancillary pairings could be integrated into a single lantern-shaped cage structure. The obvious next stage was incorporation of a third pairing, 2_{AD}:2_{DA}, to target a cage with four different low-symmetry ligands. Ligands **3** and $\mathbf{12_{AA}}$ were included as in the previous study. Ligand $\mathbf{2_{DD}2_{DA}}$ retained the capacity to pair with the 2_{AA} site of $\mathbf{12_{AA}}$, but also had a 2_{DA} site capable of interaction with the 2_{AD} site on ligand $\mathbf{2_{AD}}$ (Figure 2b). Both the 2_{DA} and 2_{AD} sites are 2-pyridyl-1,2,3-triazoles, but were designed to come together through reversal of their donor/acceptor capability. As with the other two pairings, one site was directly attached to the ligand (i.e. the 2_{DA} site of $\mathbf{2_{DD}2_{DA}}$) and the other had a 1,3-phenyl spacer ($\mathbf{2_{AD}}$), designed to create the correct respective geometries. These geometries were intended to ensure that they were positioned *cis* to each subsequent ligand, in the order **3**, $\mathbf{12_{AA}}$, $\mathbf{2_{DD}2_{DA}}$, $\mathbf{2_{AD}}$. With a third ancillary pairing now present, five equivalents of $[Pd(CH_3CN)_4](BF_4)_2$ were now required alongside the one equivalent of each of the low-symmetry ligands. Again, despite now the presence of three different pairings and four low-symmetry ligands, cage formation was relatively facile and only required heating at 40 °C for six hours. As with the previous two cages, mass spectrometry on the sample showed formation of a species with the desired composition, such as at $m/z = 1773.1781$, $[Pd_5(\mathbf{3})(\mathbf{12_{AA}})(\mathbf{2_{DD}2_{DA}})(\mathbf{2_{AD}})](BF_4)_8^{2+}$ (Supporting Information Figure S1.47). A single signal per ligand environment was again observed in the ^{1}H NMR spectrum of the complex, again confirming the formation of a single enantiomeric pair (Figure 4c). Again, ^{1}H NOESY NMR could be used to determine position and orientation of the

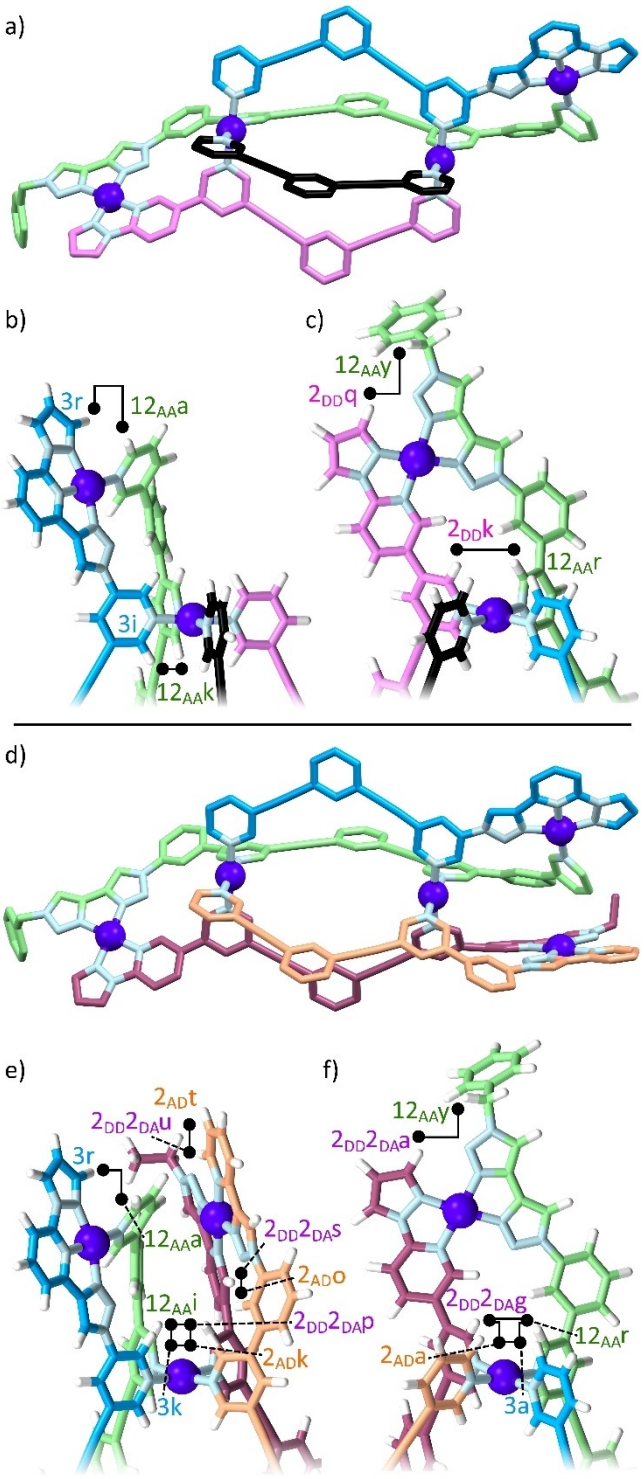

Figure 5. Representations of the DFT-calculated structures for a) $\mathbf{3{\cdot}12_{AA}{\cdot}2_{DD}{\cdot}0}$, together with close-up views (b and c) of both ends, and d) $\mathbf{3{\cdot}12_{AA}{\cdot}2_{DD}2_{DA}{\cdot}2_{AD}}$, together with close-up views (e and f) of both ends. Close-ups have NOE correlations observed by NMR spectroscopy mapped onto the structures. Ligand colours: **3** blue, $\mathbf{12_{AA}}$ green, $\mathbf{2_{DD}}$ pink, **0** black, $\mathbf{2_{DD}2_{DA}}$ maroon, $\mathbf{2_{AD}}$ orange. Nitrogen atoms are shown in light blue and palladium in dark blue. Hydrogen atoms are omitted in the main structures for clarity.

ligands (Figure 6), and be compared to the DFT calculated structure (Figure 5d, e and f). For example, **3***a* correlated to $\mathbf{12_{AA}}r$, which correlated to $\mathbf{2_{DD}2_{DA}}g$, which correlated to $\mathbf{2_{DA}}a$, which in turn correlated to **3***a*. The corresponding correlations were also observed at the other end of the cage: **3***k* to $\mathbf{12_{AA}}i$, to $\mathbf{2_{DD}2_{DA}}p$, to $\mathbf{2_{DA}}k$, in turn to **3***k*. In addition to other correlations as previously described with other cages showing proximity of 3:1 and 2_{AA}:2_{DD} pairings, the 2_{AD}:2_{DA} pairing was evidenced by correlations between environment *s* of $\mathbf{2_{DD}2_{DA}}$ and *o* of $\mathbf{2_{AD}}$, and *u* of $\mathbf{2_{DD}2_{DA}}$ and *t* of $\mathbf{2_{AD}}$, showing that all three distinct pairings had come together as intended (Figure 5e and f, Supporting Information Figures S1.51, S1.52, S1.53).

These spectral data as a whole can only be sensibly explained by the four ligands being in a single relative position and orientation, as designed. We have therefore synthesised a lantern-shaped cage with four different low-symmetry ligands, integrated into the cage with positional and orientational control.

Conclusion

The capacity to create artificial structures of greater complexity should filter through to more refined and specific function. Here, we have taken our system of complementary pairings and applied it to the generation of lantern-shaped palladium(II) cages with multiple low-symmetry ligands. The ancillary sites are only able to pair if their ligands are *cis* to one another with respect to their position on the cage, and orientated so that both sites are at the same end of the cage. This could even be accomplished with the 2_{AD}:2_{DA} homoleptic *bis*-2-pyridyl-1,2,3-triazole pairing. The 'lowest symmetry' of these cages was one with four distinct low-symmetry ligands, and control was obtained through creation of a sequence whose identity was secured through multiple pairings coming together. The combination of four different low-symmetry ligands can lead to the formation of 268 cages distinct through composition and/or isomerism (Supporting Information, excluding enantiomers). Of those, 24 are non-enantiomeric isomers of a cage composed of four different ligands, i.e. tetraleptic cages. The facile convergence on a single isomer represents a significant advance in the formation of low-symmetry architectures.

As stated earlier, this proof-of-concept study saw all ligands have simple dipyridyl 'cores' by design to ensure that structural control demonstrably originated solely from our ancillary pairings. This approach could just as easily be applied to more differentiated ligands, allowing cavity differentiation in all four quadrants, of both hemispheres. This will require the isolation of a single enantiomer as a next development, which we will target through introduction of chirality into at least one of the ligands. Also, we believe that this strategy could equally be employed to control sequence and thereby vary structure in other cage geometries as well. Furthermore, we anticipate that our pairings and similar approaches could be used to deepen complexity across a wide swathe of chemical fields.

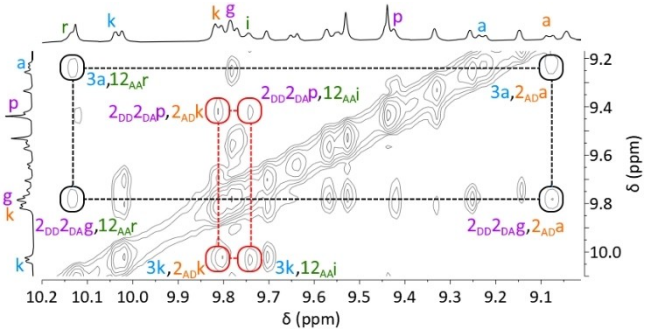

Figure 6. Partial ^{1}H 2D NOESY NMR spectrum (400 MHz, [D$_6$]DMSO, 298 K, 200 ms) of cage $\mathbf{3}\cdot\mathbf{12_{AA}}\cdot\mathbf{2_{DD}2_{DA}}\cdot\mathbf{2_{AD}}$. Label colours: **3** blue, $\mathbf{12_{AA}}$ green, $\mathbf{2_{DD}2_{DA}}$ purple, $\mathbf{2_{AD}}$ orange, **0** black. Proton labelling shown in Figure 2.

Supporting Information

The authors have cited additional references within the Supporting Information.[5a,20c,26,30]

Acknowledgements

DP acknowledges the Australian National University and the Australian Research Council (DECRA DE200100421) for funding. JDE is the recipient of an Australian Research Council Discovery Early Career Award (project number DE220100163) funded by the Australian Government. Phoenix HPC service at the University of Adelaide are thanked for providing high-performance computing resources. This research was supported by the Australian Government's National Collaborative Research Infrastructure Strategy (NCRIS), with access to computational resources provided by Pawsey Supercomputing Research Centre through the National Computational Merit Allocation Scheme. Open Access publishing facilitated by Australian National University, as part of the Wiley - Australian National University agreement via the Council of Australian University Librarians.

Conflict of Interest

The authors declare no conflict of interest.

Data Availability Statement

The data that support the findings of this study are available from the corresponding author upon reasonable request.

Keywords: Heteroleptic · Low-Symmetry · Metallosupramolecular · Palladium(II) · Self-Assembly

[1] a) T. R. Cook, P. J. Stang, *Chem. Rev.* **2015**, *115*, 7001–7045; b) K. Harris, D. Fujita, M. Fujita, *Chem. Commun.* **2013**, *49*, 6703–6712; c) N. J. Young, B. P. Hay, *Chem. Commun.* **2013**, *49*, 1354–1379; d) A. C. Pearcy, J. D. Crowley, *Chem. Eur. J.* **2023**, *29*, e202203752; e) W. Wang, Y. X. Wang, H. B. Yang, *Chem. Soc. Rev.* **2016**, *45*, 2656–2693.

[2] D. A. McMorran, P. J. Steel, *Angew. Chem. Int. Ed.* **1998**, *37*, 3295–3297.

[3] For reviews on heteroleptic lantern-shapped cages, see: a) W. M. Bloch, G. H. Clever, *Chem. Commun.* **2017**, *53*, 8506–8516; b) S. Pullen, J. Tessarolo, G. H. Clever, *Chem. Sci.* **2021**, *12*, 7269–7293; for reviews on other heteroleptic cages, see: c) D. Bardhan, D. K. Chand, *Chem. Eur. J.* **2019**, *25*, 12241–12269; d) C.-B. Tian, Q.-F. Sun, *Chem. Eur. J.* **2023**, *29*, e202300195.

[4] A. M. Johnson, R. J. Hooley, *Inorg. Chem.* **2011**, *50*, 4671–4673.

[5] a) D. Preston, J. E. Barnsley, K. C. Gordon, J. D. Crowley, *J. Am. Chem. Soc.* **2016**, *138*, 10578–10585; similarly, using picolyl groups, see: b) R. Zhu, W. M. Bloch, J. J. Holstein, S. Mandal, L. V. Schäfer, G. H. Clever, *Chem. Eur. J.* **2018**, *24*, 12976–12982.

[6] R.-J. Li, J. Tessarolo, H. Lee, G. H. Clever, *J. Am. Chem. Soc.* **2021**, *143*, 3865–3873.

[7] Y. Liu, S.-H. Liao, W.-T. Dai, Q. Bai, S. Lu, H. Wang, X. Li, Z. Zhang, P. Wang, W. Lu, Q. Zhang, *Angew. Chem. Int. Ed.* **2023**, *62*, e202217215.

[8] W. M. Bloch, Y. Abe, J. J. Holstein, C. M. Wandtke, B. Dittrich, G. H. Clever, *J. Am. Chem. Soc.* **2016**, *138*, 13750–13755.

[9] W. M. Bloch, J. J. Holstein, W. Hiller, G. H. Clever, *Angew. Chem. Int. Ed.* **2017**, *56*, 8285–8289.

[10] Other structural types have also been generated as heteroleptic, for example see: a) Q. F. Sun, S. Sato, M. Fujita, *Angew. Chem. Int. Ed.* **2014**, *53*, 13510–13513; b) S. E. Walker, S. A. Boer, T. Malcomson, M. J. Paterson, K. L. Tuck, D. R. Turner, *Chem. Commun.* **2021**, *57*, 12456–12459; c) S. Sudan, R.-J. Li, S. M. Jansze, A. Platzek, R. Rudolf, G. H. Clever, F. Fadaei-Tirani, R. Scopelliti, K. Severin, *J. Am. Chem. Soc.* **2021**, *143*, 1773–1778; d) R.-J. Li, F. Fadaei-Tirani, R. Scopelliti, K. Severin, *Chem. Eur. J.* **2021**, *27*, 9439–9445; e) R.-J. Li, A. Marcus, F. Fadaei-Tirani, K. Severin, *Chem. Commun.* **2021**, *57*, 10023–10026; f) S. Samantray, S. Krishnaswamy, D. K. Chand, *Nat. Commun.* **2020**, *11*, 880; g) C. F. Espinosa, T. K. Ronson, J. R. Nitschke, *J. Am. Chem. Soc.* **2023**, *145*, 9965–9969; h) K. Wu, B. Zhang, C. Drechsler, J. J. Holstein, G. H. Clever, *Angew. Chem. Int. Ed.* **2021**, *60*, 6403–6407; i) J. Tessarolo, H. Lee, E. Sakuda, K. Umakoshi, G. H. Clever, *J. Am. Chem. Soc.* **2021**, *143*, 6339–6344; j) S.-C. Li, L.-X. Cai, M. Hong, Q. Chen, Q.-F. Sun, *Angew. Chem. Int. Ed.* **2022**, *61*, e202204732.

[11] For a review, see: J. E. M. Lewis, J. D. Crowley, *ChemPlusChem* **2020**, *85*, 815–827.

[12] J. E. M. Lewis, A. Tarzia, A. J. P. White, K. E. Jelfs, *Chem. Sci.* **2020**, *11*, 677–683.

[13] R. A. S. Vasdev, D. Preston, C. A. Casey-Stevens, V. Martí-Centelles, P. J. Lusby, A. L. Garden, J. D. Crowley, *Inorg. Chem.* **2023**, *62*, 1833–1844.

[14] a) D. Ogata, J. Yuasa, *Angew. Chem. Int. Ed.* **2019**, *58*, 18424–18428; b) J. E. M. Lewis, *Chem. Eur. J.* **2021**, *27*, 4454–4460; c) H. Yu, J. Li, C. Shan, T. Lu, X. Jiang, J. Shi, L. Wojtas, H. Zhang, M. Wang, *Angew. Chem. Int. Ed.* **2021**, *60*, 26523–26527.

[15] The Crowley group has also accessed heterometallic lantern-shaped cages, which are as the head-to-head isomer, see: L. S. Lisboa, J. A. Findlay, L. J. Wright, C. G. Hartinger, J. D. Crowley, *Angew. Chem. Int. Ed.* **2020**, *59*, 11101–11107.

[16] J. E. M. Lewis, *Angew. Chem. Int. Ed.* **2022**, *61*, e202212392.

[17] K. Wu, E. Benchimol, A. Baksi, G. Clever, *ChemRxiv preprint* **2023**, https://doi.org/10.26434/chemrxiv-2023-5gb4q, this content is a preprint and has not been peer-reviewed.

[18] T. Abe, N. Sanada, K. Takeuchi, A. Okazawa, S. Hiraoka, *ChemRxiv preprint* **2023**, https://doi.org/10.26434/chemrxiv-2023-hht0b, this content is a preprint and has not been peer-reviewed.

[19] a) D. Preston, K. M. Patil, A. T. O'Neil, R. A. S. Vasdev, J. A. Kitchen, P. E. Kruger, *Inorg. Chem. Front.* **2020**, *7*, 2990–3001; b) J. A. Findlay, K. M. Patil, M. G. Gardiner, H. I. MacDermott-Opeskin, M. L. O'Mara, P. E. Kruger, D. Preston, *Chem. Asian J.* **2022**, *17*, e202200093.

[20] Other groups have also worked with complementarity of different forms to form low-symmetry or heteroleptic systems, for examples see: a) A. K. Chan, W. H. Lam, Y. Tanaka, K. M. Wong, V. W. Yam, *Proc. Natl. Acad. Sci. USA* **2015**, *112*, 690–695; b) R. Trokowski, S. Akine, T. Nabeshima, *Chem. Commun.* **2008**, 889–890; c) M. Naito, H. Souda, H. Koori, N. Komiya, T. Naota, *Chem. Eur. J.* **2014**, *20*, 6991–7000; d) C. Colomban, C. Fuertes-Espinosa, S. Goeb, M. Salle, M. Costas, L. Blancafort, X. Ribas, *Chem. Eur. J.* **2018**, *24*, 4371–4381; e) R. Lavendomme, T. K. Ronson, J. R. Nitschke, *J. Am. Chem. Soc.* **2019**, *141*, 12147–12158; f) M. L. Saha, N. Mittal, J. W. Bats, M. Schmittel, *Chem. Commun.* **2014**, *50*, 12189–12192; g) N. Mittal, M. L. Saha, M. Schmittel, *Chem. Commun.* **2015**, *51*, 15514–15517.

[21] a) D. Preston, P. E. Kruger, *ChemPlusChem* **2020**, *85*, 454–465; b) J. L. Algar, D. Preston, *Chem. Commun.* **2022**, *58*, 11637–11648.

[22] a) D. Preston, A. R. Inglis, A. L. Garden, P. E. Kruger, *Chem. Commun.* **2019**, *55*, 13271–13274; b) J. L. Algar, J. A. Findlay, J. D. Evans, D. Preston, *Angew. Chem. Int. Ed.* **2022**, *61*, *e202210476*.

[23] a) J. S. Buchanan, D. Preston, *Chem. Asian J.* **2022**, *17*, e202200272; b) D. Preston, *Angew. Chem. Int. Ed.* **2021**, *60*, 20027–20035.

[24] P. Liao, B. W. Langloss, A. M. Johnson, E. R. Knudsen, F. S. Tham, R. R. Julian, R. J. Hooley, *Chem. Commun.* **2010**, *46*, 4932–4934.

[25] a) D. P. August, G. S. Nichol, P. J. Lusby, *Angew. Chem. Int. Ed.* **2016**, *55*, 15022–15026; b) S. M. Jansze, K. Severin, *J. Am. Chem. Soc.* **2019**, *141*, 815–819; c) J. Wang, T. A. Young, F. Duarte, P. J. Lusby, *J. Am. Chem. Soc.* **2020**, *142*, 17743–17750.

[26] J. Jeener, B. H. Meier, P. Bachmann, R. R. Ernst, *J. Chem. Phys.* **1979**, *71*, 4546.

[27] An inspection of crystal structures from any number of the lantern-shaped cages cited elsewhere in this report can confirm this, although helical twisting can lengthen both distances, to around 3.6 (cis) and 5.0 (trans) Å see: a) R. G. DiNardi, A. O. Douglas, R. Tian, J. R. Price, M. Tajik, W. A. Donald, J. E. Beves, *Angew. Chem. Int. Ed.* **2022**, *61*, e202205701; b) S. M. Jansze, M. D. Wise, A. V. Vologzhanina, R. Scopelliti, K. Severin, *Chem. Sci.* **2017**, *8*, 1901–1908; c) W. M. Bloch, S. Horiuchi, J. J. Holstein, C. Drechsler, A. Wuttke, W. Hiller, R. A. Mata, G. H. Clever, *Chem. Sci.* **2023**, *14*, 1524–1531.

[28] Correlation strength is proportional to the inverse of nuclear separation to the power of 6. See: K. J, *Understanding NMR spectroscopy*, 2nd ed, Markono Print Media Pty, **2009**.

[29] The ^{19}F NMR spectrum of this cage indicated that the tetrafluoroborate anion was not encapsulated within the cavity or otherwise significantly interacting. This was also true for other cages investigated in this study (Supporting Information).
.

[30] a) P. Kirsch, S. C. Stein, A. Berwanger, J. Rinkes, V. Jakob, T. F. Schulz, M. Empting, *Eur. J. Med. Chem.* **2020**, *202*, 112525; b) J. Guo, Y. W. Xu, K. Li, L. M. Xiao, S. Chen, K. Wu, X. D. Chen, Y. Z. Fan, J. M. Liu, C. Y. Su, *Angew. Chem. Int. Ed.* **2017**, *56*, 3852–3856; c) Y. Domoto, M. Abe, T. Kikuchi, M. Fujita, *Angew. Chem. Int. Ed.* **2020**, *59*, 3450–3454; d) C. S. Rani, A. G. Reddy, E. Susithra, K.-K. Mak, M. R. Pichika, S. Reddymasu, M. V. B. Rao, *Med. Chem. Res.* **2021**, *30*, 74–83; e) H. C. Bertrand, M. Schaap, L. Baird, N. D. Georgakopoulos, A. Fowkes, C. Thiollier, H. Kachi, A. T. Dinkova-Kostova, G. Wells, *J. Med. Chem.* **2015**, *58*, 7186–7194; f) V. Fiandanese, D. Bottalico, G. Marchese, A. Punzi, F. Capuzzolo, *Tetrahedron* **2009**, *65*, 10573–10580; g) B. Happ, D. Escudero, M. D. Hager, C. Friebe, A. Winter, H. Gorls, E. Altuntas, L. Gonzalez, U. S. Schubert, *J. Org. Chem.* **2010**, *75*, 4025–4038; h) K. J. Kilpin, M. L. Gower, S. G. Telfer, G. B. Jameson, J. D. Crowley, *Inorg. Chem.* **2011**, *50*, 1123–1134; i) K. Stott, J. Stonehouse, J. Keeler, T.-L. Hwang, A. J. Shaka, *J. Am. Chem. Soc.* **1995**, *117*, 4199; j) A. Jerschow, N. Müller, *J. Magn. Reson. Ser. A* **1996**, *123*, 222–225; k) A. Jerschow, N. Müller, *J. Magn. Reson.* **1997**, *125*, 372–375; l) F. Neese, *Wiley Interdiscip. Rev.: Comput. Mol. Sci.* **2022**, *12*, e1606; m) J. P. Perdew, *Phys. Rev. B* **1986**, *33*, 8822–8824; n) F. Weigend, R. Ahlrichs, *Phys. Chem. Chem. Phys.* **2005**, *7*, 3297–3305; o) D. Andrae, U. Häußermann, M. Dolg, H. Stoll, H. Preuß, *Theor. Chim. Acta* **1990**, *77*, 123–141; p) S. Grimme, S. Ehrlich, L. Goerigk, *J. Comput. Chem.* **2011**, *32*, 1456–1465.

Manuscript received: September 25, 2023
Accepted manuscript online: October 10, 2023
Version of record online: October 10, 2023